Elicitation of superinfection exclusion by p28 of turnip crinkle virus is separable from its replication function with mutations at specific amino acid residues

Qin Guo[1], Shaoyan Zhang[1], Rong Sun[1], Xiaolong Yao[1], Xiao-Feng Zhang[1,2], Satyanarayana Tatineni[3], Tea Meulia[1,4], and Feng Qu[1]*

[1]Department of Plant Pathology, [4]Molecular and Cellular Imaging Center, Ohio Agricultural Research and Development Center, The Ohio State University. Wooster, OH 44691.

[2]Fujian Key Laboratory of Plant Virology, Institute of Plant Virology, Fujian Agriculture and Forestry University, Fuzhou, China

[3]USDA-ARS and Department of Plant Pathology, University of Nebraska-Lincoln, Lincoln, NE 68583

*Primary contact: Feng Qu, qu.28@osu.edu; 330-263-3835

Decoupling two opposite functions of TCV p28

ABSTRACT

We recently reported that the p28 auxiliary replication protein encoded by turnip crinkle virus (TCV) is also responsible for eliciting superinfection exclusion (SIE) against superinfecting TCV. However, it remains unresolved whether the replication function of p28 could be separated from its ability to elicit SIE. Here we report the identification of two single amino acid (aa) mutations that decouple these two functions. Using an *Agrobacterium* infiltration-based delivery system, we transiently expressed a series of p28 deletion and point mutants, and tested their ability to elicit SIE against a co-introduced TCV replicon. We found that substituting alanine (A) for valine (V) and phenylalanine (F) at p28 positions 181 and 182, respectively, modestly compromised SIE in transiently expressed p28 derivatives. Upon incorporation into TCV replicons, V181A and F182A decoupled TCV replication and SIE diametrically. While V181A impaired SIE without detectably compromising replication, F182A abolished TCV replication but had no effect on SIE once the replication of the defective replicon was restored through complementation. Both mutations diminished accumulation of p28 protein, suggesting that p28 must reach a concentration threshold in order to elicit a strong SIE. Importantly, the severe reduction of F182A protein levels correlated with a dramatic loss in the number of intracellular p28 foci formed by p28-p28 interactions. Together these findings not only decouples the replication and SIE functions of p28, but also unveils a concentration dependence for p28 coalescence and SIE elicitation. These data further highlight the role of p28 multimerization in driving the exclusion of secondary TCV infections.

34 **IMPORTANCE**

35 Superinfection exclusion (SIE) insulates virus-infected cells from subsequent invasion by the same
36 or closely related viruses. SIE has been observed in both animal and plant virus-infected cells. Therefore,
37 a thorough understanding of how SIE is achieved at the molecular level is expected to inspire novel
38 strategies for combating virus infections in humans, animals, and plants. Our group has been using
39 turnip crinkle virus (TCV) to elucidate the molecular interactions critical for SIE elicitation. The current
40 study builds on the previous observation that TCV SIE is elicited by one single TCV-encoded protein
41 (p28), and further identifies key regions and amino acids that are needed for SIE. We unravel key amino
42 acid changes that decouple the replication and SIE functions of p28, and provides novel mechanistic
43 insights of SIE.

44 **INTRODUCTION**

45 Many viruses block the subsequent entry and/or replication of the same or closely related viruses
46 in the cells they occupy, through a process known as superinfection exclusion (SIE). These viruses
47 include important human and animal pathogens such as human immunodeficiency virus (HIV), hepatitis
48 C virus (HCV), West Nile virus (WNV), and vesicular stomatitis virus (VSV) (1–5), as well as plant
49 pathogens like tobacco mosaic virus (TMV), citrus tristeza virus (CTV), cucumber mosaic virus (CMV),
50 wheat streak mosaic virus (WSMV), turnip crinkle virus (TCV) (6–11), and more recently sonchus yellow
51 net virus (12). SIE in plant virus infections is also thought to underlie the well-documented cross
52 protection phenomenon (13–15). Cross protection insulates plants from a disease-causing virus by
53 simply pre-inoculating them with a mild variant of the same virus. Although cross protection has been
54 adopted for plant virus disease management for at least 50 years (13), its underlying molecular
55 mechanism remains poorly understood.

56 A number of earlier studies investigated SIE of plant viruses by tagging the same virus with two
57 different fluorescent proteins (e.g. green fluorescent protein [GFP] and mCherry) (6, 7, 9, 10, 16, 17).
58 These studies demonstrated that most of the viruses excluded their own variants at the single cell level,
59 thus implicating intracellular exclusion as one of the primary causes for SIE. Using this approach, Zhang
60 and colleagues (16) found that SIE in TCV infections occurred inside individual cells, and it acted to block
61 the replication of the superinfecting TCV replicons. Strikingly, this replicational blockage was mediated
62 by p28, one of the TCV-encoded proteins required for TCV genome replication (16). The fact that p28,
63 the auxiliary replication protein of TCV, functions to both facilitate and repress the replication of TCV
64 genomic RNA (gRNA), along with the observation that fluorescent protein-tagged p28 formed large
65 intracellular bodies that coalesced other p28 variants, prompted the hypothesis that p28 undergoes
66 concentration-dependent conformational changes to accommodate its dual functions. Namely, the p28

67 protein assumes one conformation at lower concentrations to enable replication, but another self-
68 perpetuating conformation at higher concentrations to block replication (16, 18).
69 TCV is a small icosahedral plant virus with a (+)-strand RNA genome that encodes five proteins.
70 The 5' proximal p28 and its C-terminally extended derivative – p88 – are both translated directly from
71 TCV genomic RNA (gRNA), and are themselves required for gRNA replication (Fig. 1A). Since the
72 production of p88 depends on infrequent translational read-through of the p28 stop codon (UAG), the
73 intracellular concentration of p28 far exceeds that of p88 (19). However, p28 lacks the conserved RNA-
74 dependent RNA polymerase (RdRP) motif, is hence known as the auxiliary replication protein. On the
75 other hand, p88 is thought to be directly responsible for gRNA replication through its RdRP activity. TCV
76 additionally encodes two small movement proteins, p8 and p9, that are translated from subgenomic
77 RNA 1 (sgRNA1), and a capsid protein/silencing suppressor from sgRNA2 (Fig. 1A) (20–22).
78 In the recent study by Zhang and colleagues (16), we established that p28 was necessary and
79 sufficient to elicit SIE against a co-introduced TCV replicon, and that it likely accomplished this by
80 sequestering freshly translated p28 molecules into self-perpetuating p28 polymers. These earlier
81 observations raised at least three questions: (i) does the SIE activity of p28 require any specific domains
82 or amino acid residues in p28? (ii) can this replication-repressing SIE activity of p28 be decoupled from
83 its essential role in replication? (iii) can either of the p28 functions (replication and SIE) be decoupled
84 from the RdRP activity of p88? This last question is of interest as p88 encompasses the entire p28 at its
85 N-terminal 2/5 (Fig. 1A). The current study addresses these questions by identifying a 12 amino acid (aa)
86 region in p28 that is required for efficient SIE. Moreover, two single aa changes within this region not
87 only enabled the decoupling of SIE activity of p28 from its replication function, but also the separation of
88 the replication function of p28 from that of p88. Finally, both single aa mutations lowered the cellular
89 concentration of p28, and diminished the number of p28 inclusion bodies. Our findings unveil novel

90 mechanistic details of SIE elicitation by TCV p28, and provide powerful new tools for further elucidation
91 of TCV SIE.
92
93 **RESULTS**
94 **Deletion mutagenesis of p28-GFP fusion protein identifies a small region needed for robust SIE**
95 **elicitation**. We recently reported that a C-terminal GFP fusion bolsters the ability of p28 to elicit SIE to
96 TCV (16). Specifically, expression of the p28-GFP fusion protein in *Nicotiana benthamiana* cells abolished
97 the replication of TCV_sg2R, an mCherry-expressing TCV replicon, in the same cells, erasing the
98 replication-dependent mCherry fluorescence (16). Additionally, the strong replicational repression by
99 p28-GFP correlated with the occurrence of large, intense green fluorescent foci in these cells (16). These
100 easy-to-monitor fluorescent phenotypes prompted us to use p28-GFP as the launch pad to map domains
101 in p28 essential for SIE elicitation. To systematically screen for these domains, we generated a series of
102 in-frame deletions within the p28 portion of p28-GFP (Fig. 2A). The effect of these deletions on the SIE-
103 eliciting ability of p28 was evaluated by expressing the mutant proteins in *N. benthamiana* cells, and
104 assessing the replication of the co-introduced TCV_sg2R replicon with Northern blot hybridizations. In
105 addition, we also monitored the replication-dependent diffuse mCherry fluorescence, as well as the
106 GFP-fluorescent mutant fusion proteins, using confocal microscopy.
107 As shown in Fig. 2B, deletion of the N-terminal half of the 250-aa p28 (mutant Δ2-125) caused only
108 minimal loss in the SIE elicitation by p28-GFP, leading to a very modest recovery of TCV_sg2R replication
109 (Fig. 2A; and Fig. 2B, lanes 7 and 8). A specific N-terminal domain could not be delineated because none
110 of the smaller deletions within this region, including Δ2-36, Δ37-50, Δ37-100, Δ51-100, and Δ76-125, led
111 to detectable replication of TCV_sg2R (Fig. 2B, lanes 11-18; Fig. 2C, lanes 11-12). These results suggest
112 that, in the presence of the C-terminal GFP tag, the N-terminal half of p28 plays a modest role in SIE
113 elicitation. Consistent with this conclusion, the Δ2-100 deletion had an even smaller effect than Δ2-125

114 on SIE, leading to only occasional detection of TCV_sg2R replication (Fig. 2B, lanes 9 and 10; Fig. 2D,
115 lanes 7 and 8).

116 Interestingly, the Δ2-155 mutant, which extends the Δ2-125 deletion for just 30 aa, permitted a
117 substantially higher level of TCV_sg2R replication (Fig. 2C, compare lanes 7-8 with 9-10). However, a
118 separate deletion of the 30 aa alone (Δ126-155) had a much weaker, though consistently detected
119 release of TCV_sg2R replication (Fig. 2C, compare lanes 13, 14 with lanes 7, 8). This suggested that loss
120 of SIE activity by the mutant Δ2-155 could be attributed to the additive or synergistic effect of two
121 regions – aa 2-125 and 126-155. Nevertheless, specific SIE-eliciting sequence motifs or aa residues
122 within the first 155 aa region could not be reliably identified with the GFP-tagged constructs.

123 Surprisingly, another relatively small deletion (Δ156-190, 35 aa in total) caused a loss of SIE activity
124 that rivaled the large Δ2-155 deletion (Fig. 2C, compare lanes 15, 16 with 7 and 8), thus identifying a
125 region with a relatively strong effect. Beyond aa 190, the entire C-terminal 60-aa region could be
126 removed without detectably compromising the SIE-eliciting activity of p28-GFP (Fig. 2D, Δ191-250, lanes
127 9 and 10). Indeed, a double deletion mutant combining the Δ2-100 and Δ191-250 deletions was no
128 worse than Δ2-100 alone at repressing TCV_sg2R replication (Fig. 2D, compare lanes 13, 14 with lanes 7
129 and 8). This further confirmed that the last 60-aa region was dispensable for SIE elicitation by p28-GFP.

130 Notably, the loss of SIE activity by many of the deletion mutants was accompanied by dramatic
131 changes in the intracellular behavior of mutant proteins. For example, although the SIE loss caused by
132 the Δ2-100 deletion was minimal, the Δ2-100-GFP formed large foci in substantially fewer cells than the
133 wild-type p28-GFP (Fig. 2E, panels 3 and 4), and instead exhibited a distribution resembling soluble GFP
134 in many cells (Fig. 2E, panel 4). Nevertheless, the smaller, more numerous foci formed by the GFP-
135 tagged Δ2-125, Δ126-155, and Δ156-190 proteins appear to be consistent with a requirement for larger
136 aggregates in SIE elicitation (Fig. 2E, panels 5, 7, and 8). Further supporting this idea is the observation

137 that the Δ2-155-GFP mutant protein was predominantly diffusely distributed, suggestive of a soluble
138 protein (Fig. 2E, panel 6).

139 **Additional deletions within the aa 156-190 region identify a 12-aa stretch with a significant role**
140 **in eliciting SIE.** That a substantial loss of SIE-eliciting activity could be inflicted by a mere 35-aa deletion
141 (Δ156-190) prompted us to further interrogate this small region using the p28-GFP fusion construct. To
142 this end, three smaller deletions (Δ156-170, Δ171-182, Δ183-190, deleting 15, 12, and 8 aa, respectively)
143 were generated and the resulting deletion mutants were analyzed for their ability to elicit SIE against
144 TCV_sg2R. As shown in Fig. 3A, neither Δ156-170 (lanes 9 and 10) nor Δ183-190 (lanes 13 and 14)
145 caused detectable loss of the SIE-eliciting activities. By contrast, deletion of aa 171-182 appeared to
146 account for most of the SIE loss observed with the Δ156-190 mutant.

147 We next investigated whether this 12-aa region contained any specific aa residue(s) critical for SIE
148 elicitation by generating three consecutive 4-aa deletions. As shown in Fig. 3B, lanes 9-14, all three
149 deletion mutants compromised the SIE-eliciting activity of p28-GFP to similar extents as the 12-aa
150 deletion mutant Δ171-182 (lanes 7 and 8). Therefore, it appears that the entire 12-aa region is needed
151 for eliciting a robust SIE. We then chose the last four aa residues of this region for single aa mutagenesis
152 and changed each of them to alanine (Fig. 3B, lanes 15-22). When these single aa mutants were
153 introduced into plant cells along with the TCV_sg2R replicon, only the F182A mutant caused a barely
154 detectable accumulation of TCV_sg2R RNAs (Fig. 3B, lanes 21 and 22), suggesting that the phenylalanine
155 to alanine change weakly compromised the SIE-eliciting ability of p28-GFP.

156 Confocal microscopy showed that Δ156-170, Δ171-182, and Δ183-190 all abolished the ability to
157 form large aggregates (Fig. 3C, panels 3 and 4, also see Fig. 2E), and instead formed smaller, but more
158 numerous foci that sometimes arranged along cell boundaries. The Δ156-170 mutant was noteworthy
159 because it did allow occasional escape of red fluorescent cells, thus TCV_sg2R replication, even though
160 such low-level replication was not detected with Northern blotting (see above). This suggested that it

161 was important to use both Northern blotting and confocal microscopy to capture the full spectrum of
162 SIE-eliciting activities by these mutants.

163 Interestingly, the smaller, 4-aa deletion mutant Δ179-182 and the larger, 12-aa deletion mutant
164 Δ171-182 behaved highly similarly when inspected with confocal microscopy. Both permitted TCV_sg2R
165 replication in easily detectable numbers of cells, even though their replication levels as measured with
166 Northern blotting was much lower than controls without any p28-GFP derivatives (Fig. 2B, lanes 7-14).
167 Finally, three of the four single aa mutants, P179A, R180A, and V181A, formed large aggregates very
168 similar to those of wild-type p28-GFP, though smaller foci were also seen (Fig. 3C, panels 7-9). By
169 contrast, in cells treated with the F182A mutant, large aggregates were absent (Fig. 3C, panel 10).
170 Among these cells, replication-dependent red fluorescence was occasionally observed, thus confirming
171 the weak TCV_sg2R replication detected with Northern blotting (Fig. 2B, lanes 21-22).

172 **Replacing the C-terminal GFP with a double HA tag unveils additional regions important for SIE-**
173 **elicitation by p28**. Experiments using the p28-GFP fusion protein mutants identified the 12-aa region
174 spanning aa 171-182 as critically important for p28 to elicit SIE. But they failed to identify any other p28
175 regions that were specifically needed for SIE elicitation. These results contrasted with our previous
176 observations implicating the N-terminus of p28 in SIE elicitation. We showed earlier that fusing a short
177 G11 tag (25 aa) at the N-terminus rendered p28 incapable of eliciting SIE (16). We also found that a
178 truncated form of p28 missing the first 36 aa was no longer able to elicit SIE (16, 23). Did the C-terminal
179 GFP fusion in p28-GFP allow p28 to circumvent certain other critical regions, possibly through the
180 tendency of GFP to self-dimerize (24)? To address this question, we decided to adopt p28-HA, another
181 strong SIE-eliciting p28 variant with a C-terminal, duplicated hemagglutinin tag (16, 23). To this end, the
182 GFP in all deletion mutants described earlier was replaced with the HA tag and the resulting HA-tagged
183 mutants were retested for SIE induction.

184 As shown in Fig. 4A, the HA substitution indeed revealed a role for the N-terminal region in SIE
185 elicitation. The SIE-eliciting activity of p28-HA was not detectably weakened by deleting aa 51-100 or
186 191-250, suggesting that up to 110 amino acid residues of p28 could be removed without detectably
187 weakening SIE elicitation. However, this activity is clearly compromised by deletions of aa 2-36, 126-155,
188 and 156-190, and aa 37-100, 76-125, and 183-190 to lesser extents. Therefore, use of p28-HA as the
189 backbone permitted the identification of two additional p28 regions with potentially specific roles in SIE
190 elicitation, namely aa 2-50, and 126-155.

191 **Use of p28-HA reveals key amino acid residues within the aa 171-182 region critical for SIE**
192 **elicitation**. We next attempted to fine-map the 171-182 region, whose deletion compromised SIE in
193 both GFP and HA-tagged p28 variants, using HA-tagged mutants. As shown in Fig. 4B, use of the p28-HA
194 backbone revealed partial SIE losses caused by the Δ156-170 and Δ183-190 deletions (lanes 7, 8, 11, 12)
195 that were undetectable with the p28-GFP backbone (Fig. 3A, lanes 9, 10, and 13, 14). However, it is
196 important to note that only the deletion of the aa 171-182 core sequence fully recapitulated the
197 phenotype of the larger 156-190 deletion (Fig. 4B, compare lanes 5, 6 with 9, 10). Furthermore, each of
198 the three smaller, 4-aa deletions (Δ171-174, Δ175-178, and Δ179-182) within the aa 171-182 region
199 inflicted an SIE loss that is nearly identical to the 12-aa Δ171-182 (Fig. 4B, lanes 13-18).

200 We next re-examined the effect of four single aa substitutions using the p28-HA backbone. As
201 shown in Fig. 4C, the very weak SIE loss caused by the F182A mutation in p28-GFP background now
202 became easily detectable (lanes 15 and 16). Indeed, only the R180A mutation failed to inflict a
203 meaningful loss in the SIE-eliciting activity of p28-HA (lanes 11 and 12). By contrast, both P179A and
204 V181A mutations correlated with weak losses in SIE elicitation, with P179A being slightly less disruptive
205 than V181A (lanes 9, 10, 13 and 14).

206 **TCV replicons containing the V181A mutation overcome SIE in a substantial fraction of cells**. We
207 next wondered whether the single-aa mutations that compromised SIE in transiently expressed p28-GFP

208 and p28-HA had similar effects in TCV replicons. To resolve this question, we introduced the V181A and
209 F182A mutations into TCV_sG6H and TCV_sg2R, two TCV replicons that encode GFP [sG6H denotes GFP
210 with an N-terminal 6XHis tag (25)] and mCherry in place of CP, respectively (Fig. 1). These replicons were
211 then tested in co-infected cells to determine whether the mutations compromised SIE of TCV.

212 Although the GFP-encoding replicon (TCV_sG6H) appeared to replicate less robustly, and
213 produced much less sgRNAs (Fig. 5A, lane 2), it produced easily detectable green fluorescence (Fig. 5B,
214 top left), probably due to translational initiation from an internal ribosomal entry site identified recently
215 (26). Replicons with the V181A mutation (V181A_sG6H and V181A_sg2R) replicated to levels
216 comparable to wild-type replicons encoding wild-type p28 (and p88) (Fig. 5A, compare lanes 4, 5 with 2,
217 3, respectively). By contrast, the F182A mutation abrogated TCV replication to levels below the
218 detection limit of Northern blotting (lanes 6 and 7). Next, the V181A replicons were subjected to co-
219 infection experiments to assess the levels of SIE. As shown in Fig. 5B, while wild-type replicons exhibited
220 strong SIE that precluded the co-expression of GFP and mCherry in the same cells (top row), the V181A
221 replicons permitted such co-expression in approximately 19% of green- or red-fluorescent cells. These
222 results demonstrated that the same V181A mutation that compromised the ability of p28-HA to repress
223 TCV replication also compromised the ability of p28 to elicit SIE in TCV replicons.

224 **The F182A mutation disrupts the replication function of p28 but not p88**. The impact of the
225 F182A mutation on replicon SIE could not be readily examined because it abolished TCV replication
226 when incorporated in replicons (Fig. 5). Since the p28 coding sequence is shared by p88 in the replicon
227 context, the F182A change could have disrupted the replication function of p28, or p88, or both. To
228 resolve this issue, we attempted to complement the replication of the F182A_sg2R replicon using
229 transiently expressed, tag-free p28 and p88 (Fig. 1B). As shown in Fig. 6A, F182A_sg2R replication was
230 restored to easily detectable levels by transiently expressed p28 (compare lanes 9, 10 to 5, 6), but not
231 p88 (lanes 13 and 14). Therefore, the F182A mutation primarily disrupted the auxiliary replication

232 function of p28. While minor perturbation of p88 function by F182A could not be ruled out, such
233 perturbation did not abolish TCV replication. Taken together, the F182A mutation severely debilitated
234 the replication function of p28, but not p88. In conclusion, this mutation decouples the replication
235 functions of p28 and p88.

236 **An F182A-containing replicon, upon replicational complementation, exerts robust SIE against a**
237 **wild-type replicon.** We next examined whether the replicational defect of the F182A-containing
238 replicons could be complemented by another replicon encoding a replication-competent p28, and
239 whether the p28(F182A) protein produced by the complemented replicon might exert SIE against the
240 replicon that provided the complementing p28. To answer this question, we paired the F182A_sg2R
241 replicon with TCV_sG6H or V181A_sG6H, in co-infections of *N. benthamiana* cells. As shown in Fig. 6B,
242 panels 4 and 6, both TCV_sG6H and V181A_sG6H replicons complemented the F182A defect, enabling
243 an approximately ten-fold increase in the number of cells replicating F182A_sg2R (Fig. 6B, panels 3, 4,
244 and 6; Fig. 6C, red bars in groups 3, 4, and 6).

245 However, complementation by the two GFP-encoding replicons led to starkly different SIE
246 phenotypes. The complementation by TCV_sG6H, which encodes a wild-type p28, gave rise to mCherry-
247 expressing cells that never contained GFP fluorescence (Fig. 6B, panel 4; Fig. 6C, group 4). Conversely,
248 the GFP-expressing cells also never contained mCherry. Because the TCV_sG6H construct must reside in
249 the same cells as the F182A_sg2R construct in order to supply the replication-complementing wild-type
250 p28, these observations strongly suggested that the p28(F182A) protein, now produced by the
251 replicating F182A_sg2R replicon, exerted a powerful SIE to block TCV_sG6H replication. Note that we
252 have shown in a previous study (16) that commencement of TCV replication in different agro-infiltrated
253 *N. benthamiana* cells was highly asynchronous, meaning many cells could translate wild-type p28
254 protein from the 2X35S-driven replicon transcripts, but fail to immediately embark on replicon

255 replication. These cells would provide the p28 protein to complement the replication of F182A_sg2R,
256 the latter then turn around to exert SIE against the p28-providing wild-type replicon.
257 The assertion that both F182A_sg2R and TCV_sG6H constructs must have been present in those
258 red fluorescent cells is further bolstered by the contrasting SIE phenotype observed from the
259 complementation mediated by V181A_sG6H (Fig. 6B, panel 6; Fig. 6C), as these experiments were
260 carried out in parallel. Specifically, when the replication of F182A_sg2R was complemented with the
261 V181A_sG6H replicon, approximately one half of the red fluorescent cells also contained GFP
262 fluorescence. This probably reflected the partial loss of SIE-eliciting capacity by the p28(V181A) protein
263 (Fig. 5B. Also see Fig. 6B, panel 5). But this result also demonstrated that two different replicon
264 constructs readily entered the same agro-infiltrated cells. Together these results indicated that when
265 expressed from a replicating replicon, the p28(F182A) protein is fully capable of exerting a strong SIE
266 against another replicon in the same cells, despite its inability to facilitate replication on its own.
267 Therefore, in addition to decoupling the replication function of p28 and p88, the F182A mutation also
268 decoupled the SIE function and replication function of p28 – but in a manner diametrical to the V181A
269 mutation.
270 **The p28(V181A) and p28(F182A) mutant proteins accumulated to substantially lower levels in**
271 **cells, and formed fewer p28 foci**. Why did the V181A mutation weaken SIE in both transiently expressed
272 p28 proteins and TCV replicons, whereas F182A did so only in transiently expressed p28? To address this
273 question, we assessed the accumulation levels of the mutant p28 proteins using Western blotting. We
274 chose to assay the GFP and HA-tagged forms of p28 because a p28-specific antibody is not yet available
275 despite repeated attempts using multiple vendors. As shown in Fig. 7A and B, both GFP and HA-tagged
276 forms of V181A and F182A mutant p28 accumulated to levels substantially lower that their wildtype p28
277 counterparts. Importantly, while the HA-tagged forms of both mutant proteins diminished to levels
278 below the detection limit (Fig. 7B), the GFP-tagged forms showed a slight difference between the two,

279 with V181A, but not F182A, being marginally detectable. These results suggested that both mutations
280 compromised p28 accumulation, but the effect of F182A was more pronounced.

281 To further investigate how these two mutants handicapped SIE, we adopted a low-background bi-
282 fluorescence complementation (BIFC) assay (27, 28) to examine the inter-molecular interactions among
283 the mutant p28 proteins. This improved BIFC assay used a monomeric Venus (mVenus) protein that is
284 split between the 10th and 11th (the last) β-strands to minimize self-association between the untagged
285 fragments of this fluorescent protein, hence drastically reducing false positives. An additional advantage
286 of this new system is that the large N-terminal mVenus fragment (NVen, 10 β-strands) could be readily
287 detected using a GFP antibody. To prepare for the BIFC assay, the V181A and F182A mutants of p28,
288 along with wildtype p28, were fused to the N-termini of NVen and CVen (the 11th β-strand of mVenus).
289 The resulting binary constructs were delivered into *N. benthamiana* cells to detect potential
290 intermolecular interactions. As a negative BIFC control, we paired the NVen-tagged p28 with CVen-
291 tagged p60 – a deletion mutant of p88 with its N-terminal p28 portion removed. p28 and p60 did not
292 interact with each other in preliminary BIFC assays (also see later).

293 To ensure the constructs expressed the intended proteins, we first examined the accumulation
294 levels of the NVen-tagged proteins (the CVen tagged forms could not be detected due to the small size
295 of the tag). As shown in Fig. 7C, the wildtype p28-NVen accumulated to very high levels in the presence
296 of p28-CVen, but to a much more modest level in the presence of p60-CVen (lanes 2 and 3), suggesting
297 that it was stabilized by p28-p28 interactions (see later). Consistent with the results of Figs. 7A and B,
298 substantially reduced accumulation was observed with both V181A-NVen and F182A-NVen proteins, and
299 the reduction was more dramatic for F182A-NVen (Fig. 7C, lanes 4 and 5). Compared to the p28-
300 NVen/p60-CVen negative control (lane 3), the p28-NVen protein was slightly increased by V181A-CVen
301 but modestly reduced by F182A-CVen (lanes 6 and 8). Notably, presence of p28-CVen did not enhance

302 the accumulation of either V181A-NVen or F182A-NVen (lanes 7 and 9), suggesting that their levels were
303 regulated independently of the presence of wildtype p28.
304 When viewed under a confocal microscope, the p28-NVen/p28-CVen pair gave rise to intensely
305 bright yellow foci that resembled the p28-GFP foci (Fig. 7D, panel 2). By contrast, the p28-NVen/p60-
306 CVen pair was completely devoid of any yellow fluorescent signals, indicating an absence of p28-p60
307 interaction (panel 3). Interestingly, V181A-NVen/V181A-CVen still interacted to form foci in easily
308 detectable, but visibly fewer numbers (panel 4). By contrast, the F182A-NVen/F182A-CVen co-delivery
309 resulted in substantially fewer foci that were mostly smaller and dimmer (panel 5). However, pairing
310 F182A-CVen with p28-NVen, or vice versa, partially restored the formation of bright yellow foci (panels 8
311 and 9). This experiment was repeated multiple times with similar results. The number of foci in each of
312 the interactions was then quantified by counting the foci in multiple equal sized leaf sections containing
313 40-50 cells (see Materials and Methods for details), and plotting the counts on box plots (Fig. 7E). The
314 quantification revealed that the V181A mutant proteins interacted with each other (Group #4), or
315 wildtype p28 (Groups #6 and 7), to yield modestly fewer fluorescent foci than p28/p28 interactions
316 (approximately 20% reduction). By contrast, the F182A/F182A interaction led to a reduction of
317 approximately 80% in focus numbers (Group #5). Notably, this reduction was partially reversed by
318 changing one of the interacting partners to a wildtype p28 derivative (Groups #8 and 9). Thus, the F182A
319 mutant proteins interacted with each other very inefficiently, probably due to low protein
320 concentrations, but were able to coalesce with the nucleated core formed by wildtype p28 to produce
321 the large foci detectable with confocal microscopy. Importantly, the lower protein levels of V181A and
322 F182A mutant p28 proteins, coupled with reduced numbers of p28 foci, strongly correlated with the
323 weakened SIE elicitation by these mutant proteins.
324
325 **DISCUSSION**

326 SIE protects host cells from being sequentially infected by the same virus. Although use of SIE in
327 controlling plant virus diseases has been extensively documented, its underlying molecular mechanism,
328 and evolutionary rationale, remain poorly understood (14). Using the model virus TCV, we have
329 previously established that SIE occurred inside individual super-invaded cells, and acted to repress the
330 replication of the superinfecting viral genomes (16, 29). We further discovered that SIE in TCV infections
331 is mediated by a single TCV-encoded protein, the p28 auxiliary replication protein, likely through the
332 formation of a self-perpetuating polymeric state that sequesters homologous p28 monomers. This
333 model raised the possibility that SIE exists to ensure that progeny genomes of a virus are excluded from
334 additional rounds of replication, thus minimizes error accumulation within single cells (18). By extension,
335 cells invaded by many copies of the same virus simultaneously, frequently in the form of collective
336 infectious units (30–33), likely also experience similar molecular events that ensure only a small number
337 of the entered genomes is allowed to replicate, and be subjected to cellular level selections. If this is
338 true, then viral mutants that weaken SIE are expected to relax this restriction, allowing more viral
339 genomes to replicate for multiple cycles in the same cells, causing fast error accumulation in viral
340 populations, and probably swift collapse of these populations.
341 The current study was designed to test the predictions of our working hypothesis by first
342 identifying mutations within TCV p28 that compromise SIE. Our systematic deletion mutagenesis of p28,
343 using two different C-terminally tagged forms of p28 as the backbones, allowed us to narrow down the
344 SIE-eliciting activity of p28 to three regions: aa 2-50, 126-155, and 156-190. The aa 156-190 region was
345 then further interrogated because deletion of this region caused a consistent loss of SIE in both p28-GFP
346 and p28-HA backgrounds. These efforts ultimately led to the identification of two amino acid residues,
347 namely valine (V) and phenylalanine (F) at positions 181 and 182, respectively, whose replacement by
348 alanine (A) in replicons led to the decoupling of p28 replication function and its SIE elicitation function. It

349 is interesting to note that these two residues appear to have different levels of conservation, with F182,
350 but not V181, being highly conserved among the p28 analogs of multiple carmoviruses (not shown).
351 The lower protein levels of p28(V181A) correlated with weak SIE in both transient expressions and
352 TCV replicons, suggesting that a protein concentration threshold had to be reached for p28 to elicit a
353 robust SIE. This is consistent with the model proposed by us in earlier studies (16, 18). Why did the
354 F182A mutant proteins, being even less abundant than V181A proteins, interfere with SIE elicitation only
355 in the transiently expressed form, but not in replicons? The answer might lie in the inability of the
356 F182A-containing replicon to replicate by itself. Specifically, replication of the F182A mutant replicon
357 must rely on wildtype (or V181A) p28 encoded by a different replicon (Fig. 6), and occurred in a small
358 number of cells (approximately 5%). In these cells, wildtype p28 protein was translated from the primary
359 transcripts of the replicon construct, but the replication of the wildtype replicon was delayed (16). This
360 delay created a precious window for the F182A mutant replicon to initiate replication with borrowed
361 wildtype p28. Once succeeding in replicating itself, the F182A mutant p28 would be produced in massive
362 amounts, thus neutralizing the lower accumulation levels. More importantly, the presence of wildtype
363 p28 in these cells would facilitate the multimerization of p28 to form nucleation cores onto which the
364 F182A p28 could coalesce, forming the large p28 foci that exert strong SIE. Indeed our BIFC experiments
365 illustrated that the low self-interaction efficiency of the p28(F182A) protein was drastically improved
366 when one of the interacting partners was changed to wildtype p28 (Fig. 7D). This scenario does not
367 apply to the V181A mutation because the V181A replicon is capable of replicating itself. Replication of
368 the V181A replicon could occur in some cells before the wildtype p28 translated from a co-introduced
369 wildtype replicon reaches the SIE-eliciting concentration threshold. Conversely, wildtype TCV could still
370 replicate in a fraction of these cells because the V181A mutant p28 protein could only exert SIE
371 inefficiently.

372 To summarize, the current study identifies two single aa mutations in TCV p28 that differentially
373 impaired the two opposite functions of p28 – replication and SIE elicitation, hence decoupling these two
374 functions of p28. These mutations will allow us to investigate the impact of SIE in the rate of mutation
375 accumulation in TCV populations, providing insights regarding the evolutionary rationale for preserving
376 SIE functionality in virus infections. These investigations would in turn unravel potential targets for
377 antiviral therapy, and prompt novel management strategies for virus diseases.
378

379 **MATERIALS AND METHODS**

380 **Constructs**. Constructs 2X35S::TCV_sg2R, p28-HA, p28 (tag-free), and Core35S::p88 (tag-free)
381 were described in previous studies (16, 23). The 2X35S::p28-GFP construct was a slightly modified
382 version of the previous p28-GFP. The new version replaced the NotI site (GCGGCCGCA) linking p28 and
383 GFP coding sequences with a BamHI site plus three additional nts (GGATCCGGA). Nearly all deletion
384 mutants, as well as single aa substitution mutants, were generated using synthetic gBlocks fragments
385 (IDT, Coralville, IA) that were integrated into various backbone plasmids (e.g. p28-GFP, p28-HA, or
386 TCV_sg2R) using Gibson Assembly cloning (NEB, Ipswich, MA). The identities of all new constructs were
387 verified with Sanger sequencing. The constructs for the BIFC assay were assembled by fusing the NVen
388 and CVen fusion tags to the C-termini of p28, p28(V181A), and p28(F182A), using as the 2X35S::p28-GFP
389 construct backbone. The cDNA sequence of NVen and CVen was derived from the paper of Gookin and
390 Assman (28).

391 **Agro-infiltration**. Upon verification, all of the constructs were introduced into *Agrobacterium*
392 *tumefaciens* strain C58C1 with electroporation (34, 35). To carry out the experiments described in the
393 Results section, various combinations of *Agrobacterium* suspensions were mixed together and delivered
394 into *N. benthamiana* leaves as described (23, 29, 34, 36). A p19-expressing *Agrobacterium* strain was
395 included in all combinations to alleviate RNA silencing-mediated mRNA degradation.

396 **RNA extraction and Northern blotting**. Total RNA was extracted from agro-infiltrated *N.*
397 *benthamiana* leaves using the Direct-zol RNA Miniprep kit (Zymo Research, Irvine, CA). To ensure
398 consistency, four equivalent leaf sections derived from infiltrated leaves of four different plants were
399 pooled before RNA extraction. The RNA extraction procedure included a DNase treatment step that
400 removes DNA contamination. The RNA was then quantified with NanoDrop and subjected to Northern
401 blotting as described (23, 29, 34, 36).
402 **Protein extraction and Western blotting**. Proteins were extracted from the agro-infiltrated N.
403 benthamiana leaves following the protocol of Zhang et al (22). The polyclonal GFP and the monoclonal
404 HA antibodies were purchased from Invitrogen. The AP-conjugated anti-rabbit (GFP) and anti-mouse
405 (HA) secondary antibodies were purchased from Pierce and Novus, respectively. The HRP-conjugated
406 anti-rabbit (GFP) secondary antibody was purchased from Abcam.
407 **Confocal microscopy and quantification of fluorescent cells.** Confocal microscopic observations
408 were carried out using a Leica Confocal microscope (TCS SP5) available at Molecular and Cellular Imaging
409 Center at the Ohio Agricultural Research and Development Center, The Ohio State University. To
410 quantify the percentage of cells expressing GFP, mCherry, or reconstituted mVenus (Fig. 5 and 7), the
411 agro-infiltrated *N. benthamiana* leaf sections were photographed under the confocal microscope, at the
412 low magnification (10X), and for three separate channels (GFP/mVenus, mCherry, and merged). For each
413 treatment, five independent leaf sections were photographed, resulting in 15 images. These images,
414 typically encompassing 40-50 cells, were then divided into 100 equal subdivisions with the grid line
415 feature of the PhotoShop software. Subdivisions that are more than 50% filled with a given fluorescence
416 (GFP, mCherry, or both) were counted as positive for the respective protein, the total counts of which
417 represent a percentage in a given image. For each treatment five counts were obtained, and standard
418 deviation were computed using these counts. In the case of BIFC experiments, the number of cells in
419 each of the selected leaf section was estimated using a co-expressed ER-mCherry protein (not shown).

420 The reconstituted mVenus foci was counted for each of the five leaf sections, and the counts were
421 quantified using box plots.
422
423 **FIGURE LEGENDS**
424 **Figure 1.** TCV genome organization, and the configurations of the constructs used in this study. **A:**
425 the organization of the 4,054 nt single-stranded, positive sense (+) TCV genome. The various boxes with
426 labels within (e.g. p28, p88, p8, p9, p38) denote the proteins encoded by the TCV genome, with the
427 boundaries of some ORFs shown. The three 3' proximal proteins (p8, p9, and p38) are translated from
428 two subgenomic RNAs (sgRNA1 and 2). **B**: representative constructs used in this study. Most constructs
429 were equipped with the strong 35S promoter with the enhancer duplicated (2X35S) in order to ensure
430 efficient transcription. Only the last, p88-expressing construct was driven by the relatively weak core
431 35S promoter as high level of p88 translation was shown to repress TCV replication (23). The top most
432 construct is a replicon shown previously to launch TCV replication in plant cells, leading to mCherry
433 expression from the sgRNA2 (20, 36). All other constructs direct transient expression of the respective
434 proteins in the absence of TCV replication.
435 **Figure 2**. Deletion mutagenesis on the p28-GFP backbone identifies the aa 156-190 region as
436 needed for robust SIE. **A**: diagrams of deletion mutants of p28-GFP showing their respective deleted
437 regions. **B, C, D:** Northern blotting results showing the levels of replicational repression imposed on the
438 TCV_sg2R replicon by p28-GFP and its deletion mutants. The p19 silencing suppressor was included to
439 mitigate the impact of RNA silencing. The double loadings represented two independent samples
440 extracted from different leaves. The positions of gRNA, sgRNA1 and 2 were highlighted with arrows (g,
441 sg1, sg2). EB: ethidium bromide-stained gel. **E:** confocal images of *N. benthamiana* leaf cells treated with
442 select p28-GFP deletion mutants along with the TCV_sg2R replicon.

443 **Figure 3**. Mapping the aa 156-190 region of p28-GFP with smaller deletions and single aa
444 exchanges identifies aa 171-182 as the key determinant of SIE. **A and B**: Northern blots showing the
445 levels of replicational repression imposed on the TCV_sg2R replicon by various smaller deletion and
446 single aa mutants of p28-GFP. **C:** confocal images of *N. benthamiana* leaf cells treated with select p28-
447 GFP mutants along with the TCV_sg2R replicon.

448 **Figure 4.** Use of the p28-HA backbone reveals additional regions contributing to SIE elicitation by
449 p28. All panels are Northern blots showing the levels of replicational repression imposed on the
450 TCV_sg2R replicon by various mutants of p28-HA.

451 **Figure 5**. Replication and SIE of mutant replicons with the V181A and F182A mutations. **A:**
452 Northern blot showing the replication (lanes 4-7) and SIE (lanes 10-13) of the mutant replicons encoding
453 different fluorescent proteins (GFP or mCherry). **B:** confocal images showing robust SIE between two
454 wild-type replicons (top panels), and the partially compromised SIE between the two V181A mutant
455 replicons. The quantification was based on five independent leaf areas each containing 40-50 cells. See
456 Materials and Methods for details. G = GFP-fluorescent cells, R = mCherry-fluorescent cells, G+R = cells
457 containing both GFP and mCherry.

458 **Figure 6**. In replicons, the F182A mutation selectively abrogates the replication function of p28,
459 but not its ability to elicit SIE. **A:** Northern blot showing that the replicational defect of the F182A
460 replicon was complemented by transiently expressed p28 but not p88. **B:** confocal images showing that
461 the replicational defect of the F182A replicon was also complemented by co-introduced wild-type and
462 V181A replicons, and the successfully complemented F182A replicon exerted robust SIE against the wild-
463 type replicon. **C:** quantification of replicational complementation and SIE of the F182A replicon. The
464 numbering of the bar groups corresponds to that of Fig. 6B panels. In all sets leaf areas of the same size,
465 containing 40-50 cells each, were chosen from five different leaves and counted for cells with different
466 fluorescence (GFP, mCherry, or both).

467 **Figure 7**. The V181A and F182A mutations reduce the level of transiently expressed p28 proteins, and
468 the number of polymeric foci formed by interacting p28 proteins. **A:** Western blot showing accumulation
469 levels of GFP-tagged wildtype p28 protein and its V181A and F182A mutants. **B:** Western blot showing
470 accumulation levels of HA-tagged wildtype p28 protein and its V181A and F182A mutants. **C:** Western
471 blot showing the accumulation levels of NVen-tagged p28, p28)V181A), p28(F182A), in the presence of
472 various CVen-tagged interaction partners. **D.** Confocal images of multimeric p28 foci formed through
473 p28-p28 interactions, visualized using mVenus-based BIFC. The numbering of the panels corresponds to
474 that of lanes in Fig. 7C. **E.** Quantification of the number of p28 foci observed in various BIFC
475 combinations. See Materials and Methods for details of quantification methods. The numbering of the
476 groups corresponds to that of lanes in Fig. 7C, and panels in Fig. 7D.
477

478 **ACKNOWLEDGMENTS**

479 We thank the labs of Drs. Lucy Stewart and Peg Redinbaugh for generous equipment sharing, and
480 other members of the Qu lab for stimulating discussions. This study was supported by a grant from the
481 National Science Foundation (#1758912), a SEEDS grant from the Ohio Agricultural Research and
482 Development Center, Graduate Assistantships from OSU and OARDC to Q.G. and R.S., respectively, as
483 well as tuition assistances to S.Z., R.S., and Q.G. from the Department of Plant Pathology, OSU.
484

485 **LITERATURE**

486 1. Nethe M, Berkhout B, van der Kuyl AC. 2005. Retroviral superinfection resistance. Retrovirology
487 2:52.

488 2. Schaller T, Appel N, Koutsoudakis G, Kallis S, Lohmann V, Pietschmann T, Bartenschlager R. 2007.
489 Analysis of Hepatitis C Virus Superinfection Exclusion by Using Novel Fluorochrome Gene-Tagged
490 Viral Genomes. J Virol 81:4591.

491 3. Tscherne DM, Evans MJ, von Hahn T, Jones CT, Stamataki Z, McKeating JA, Lindenbach BD, Rice
492 CM. 2007. Superinfection exclusion in cells infected with hepatitis C virus. J Virol 81:3693–3703.

493 4. Zou G, Zhang B, Lim P-Y, Yuan Z, Bernard KA, Shi P-Y. 2009. Exclusion of West Nile Virus
494 Superinfection through RNA Replication. J Virol 83:11765.

495 5. Simon KO, Cardamone JJ, Whitaker-Dowling PA, Youngner JS, Widnell CC. 1990. Cellular
496 mechanisms in the superinfection exclusion of vesicular stomatitis virus. Virology 177:375–379.

497 6. Julve JM, Gandía A, Fernández-del-Carmen A, Sarrion-Perdigones A, Castelijns B, Granell A, Orzaez
498 D. 2013. A coat-independent superinfection exclusion rapidly imposed in Nicotiana benthamiana
499 cells by tobacco mosaic virus is not prevented by depletion of the movement protein. Plant Mol
500 Biol 81:553–564.

501 7. Dietrich C, Maiss E. 2003. Fluorescent labelling reveals spatial separation of potyvirus populations
502 in mixed infected Nicotiana benthamiana plants. J Gen Virol 84:2871–2876.

503 8. Bergua M, Zwart MP, El-Mohtar C, Shilts T, Elena SF, Folimonova SY. 2014. A viral protein mediates
504 superinfection exclusion at the whole-organism level but is not required for exclusion at the
505 cellular level. J Virol 88:11327–11338.

506 9. Miyashita S, Kishino H. 2010. Estimation of the size of genetic bottlenecks in cell-to-cell movement
507 of soil-borne wheat mosaic virus and the possible role of the bottlenecks in speeding up selection
508 of variations in trans-acting genes or elements. J Virol 84:1828–1837.

509 10. Takahashi T, Sugawara T, Yamatsuta T, Isogai M, Natsuaki T, Yoshikawa N. 2007. Analysis of the
510 Spatial Distribution of Identical and Two Distinct Virus Populations Differently Labeled with Cyan
511 and Yellow Fluorescent Proteins in Coinfected Plants. Phytopathology 97:1200–1206.

512 11. Folimonova SY. 2012. Superinfection Exclusion Is an Active Virus-Controlled Function That Requires
513 a Specific Viral Protein. J Virol 86:5554.

514 12. Zhou X, Sun K, Zhou X, Jackson AO, Li Z. 2019. The matrix protein of a plant rhabdovirus mediates
515 superinfection exclusion by inhibiting viral transcription. J Virol JVI.00680-19.

516 13. Ziebell H, Carr JP. 2010. Cross-Protection, p. 211–264. *In* Advances in Virus Research. Elsevier.

517 14. Zhang X-F, Qu F. 2016. Cross Protection of Plant Viruses: Recent Developments and Mechanistic
518 Implications, p. 241–250. *In* Wang, A, Zhou, X (eds.), Current Research Topics in Plant Virology.
519 Springer International Publishing, Cham.

520 15. Folimonova SY. 2013. Developing an understanding of cross-protection by Citrus tristeza virus.
521 Front Microbiol 4:76.

522 16. Zhang X-F, Sun R, Guo Q, Zhang S, Meulia T, Halfmann R, Li D, Qu F. 2017. A self-perpetuating
523 repressive state of a viral replication protein blocks superinfection by the same virus. PLOS Pathog
524 13:e1006253.

525 17. Tatineni S, French R. 2016. The Coat Protein and NIa Protease of Two Potyviridae Family Members
526 Independently Confer Superinfection Exclusion. J Virol 90:10886–10905.

527 18. Zhang X-F, Zhang S, Guo Q, Sun R, Wei T, Qu F. 2018. A New Mechanistic Model for Viral Cross
528 Protection and Superinfection Exclusion. Front Plant Sci 9.

529 19. White KA, Skuzeski JM, Li W, Wei N, Morris TJ. 1995. Immunodetection, Expression Strategy and
530 Complementation of Turnip Crinkle Virus p28 and p88 Replication Components. Virology 211:525–
531 534.

532 20. Cao M, Ye X, Willie K, Lin J, Zhang X, Redinbaugh MG, Simon AE, Morris TJ, Qu F. 2010. The Capsid
533 Protein of Turnip Crinkle Virus Overcomes Two Separate Defense Barriers To Facilitate Systemic
534 Movement of the Virus in Arabidopsis. J Virol 84:7793–7802.

535 21. Zhang X, Zhang X, Singh J, Li D, Qu F. 2012. Temperature-Dependent Survival of Turnip Crinkle
536 Virus-Infected Arabidopsis Plants Relies on an RNA Silencing-Based Defense That Requires DCL2,
537 AGO2, and HEN1. J Virol 86:6847–6854.

538 22. Qu F, Ye X, Morris TJ. 2008. Arabidopsis DRB4, AGO1, AGO7, and RDR6 participate in a DCL4-
539 initiated antiviral RNA silencing pathway negatively regulated by DCL1. Proc Natl Acad Sci
540 105:14732–14737.

541 23. Zhang S, Sun R, Guo Q, Zhang X-F, Qu F. 2019. Repression of turnip crinkle virus replication by its
542 replication protein p88. Virology 526:165–172.

543 24. Shaner NC, Steinbach PA, Tsien RY. 2005. A guide to choosing fluorescent proteins. Nat Methods
544 2:905–909.

545 25. Powers JG, Sit TL, Qu F, Morris TJ, Kim K-H, Lommel SA. 2008. A Versatile Assay for the
546 Identification of RNA Silencing Suppressors Based on Complementation of Viral Movement. Mol
547 Plant Microbe Interact 21:879–890.

548 26. May J, Johnson P, Saleem H, Simon AE. 2017. A Sequence-Independent, Unstructured Internal
549 Ribosome Entry Site Is Responsible for Internal Expression of the Coat Protein of Turnip Crinkle
550 Virus. J Virol 91:e02421-16.

551 27. Kodama Y, Hu C-D. 2010. An improved bimolecular fluorescence complementation assay with a
552 high signal-to-noise ratio. BioTechniques 49:793–805.

553 28. Gookin TE, Assmann SM. 2014. Significant reduction of BiFC non-specific assembly facilitates in
554 planta assessment of heterotrimeric G-protein interactors. Plant J 80:553–567.

555 29. Zhang X-F, Guo J, Zhang X, Meulia T, Paul P, Madden LV, Li D, Qu F. 2015. Random Plant Viral
556 Variants Attain Temporal Advantages During Systemic Infections and in Turn Resist other Variants
557 of the Same Virus. Sci Rep 5.

558 30. Chen Y-H, Du W, Hagemeijer MC, Takvorian PM, Pau C, Cali A, Brantner CA, Stempinski ES,
559 Connelly PS, Ma H-C, Jiang P, Wimmer E, Altan-Bonnet G, Altan-Bonnet N. 2015.
560 Phosphatidylserine Vesicles Enable Efficient En Bloc Transmission of Enteroviruses. Cell 160:619–
561 630.

562 31. Mirabelli C, Wobus CE. 2018. All Aboard! Enteric Viruses Travel Together. Cell Host Microbe
563 24:183–185.

564 32. Andreu-Moreno I, Sanjuán R. 2018. Collective Infection of Cells by Viral Aggregates Promotes Early
565 Viral Proliferation and Reveals a Cellular-Level Allee Effect. Curr Biol 28:3212-3219.e4.

566 33. Miyashita S, Ishibashi K, Kishino H, Ishikawa M. 2015. Viruses Roll the Dice: The Stochastic Behavior
567 of Viral Genome Molecules Accelerates Viral Adaptation at the Cell and Tissue Levels. PLOS Biol
568 13:e1002094.

569 34. Qu F, Ren T, Morris TJ. 2003. The Coat Protein of Turnip Crinkle Virus Suppresses
570 Posttranscriptional Gene Silencing at an Early Initiation Step. J Virol 77:511–522.

571 35. Qu F, Ye X, Hou G, Sato S, Clemente TE, Morris TJ. 2005. RDR6 Has a Broad-Spectrum but
572 Temperature-Dependent Antiviral Defense Role in Nicotiana benthamiana. J Virol 79:15209–
573 15217.

574 36. Zhang X-F, Sun R, Guo Q, Zhang S, Meulia T, Halfmann R, Li D, Qu F. 2017. A self-perpetuating
575 repressive state of a viral replication protein blocks superinfection by the same virus. PLOS Pathog
576 13:e1006253.

577

578

Guo et al., 2019 Fig. 1

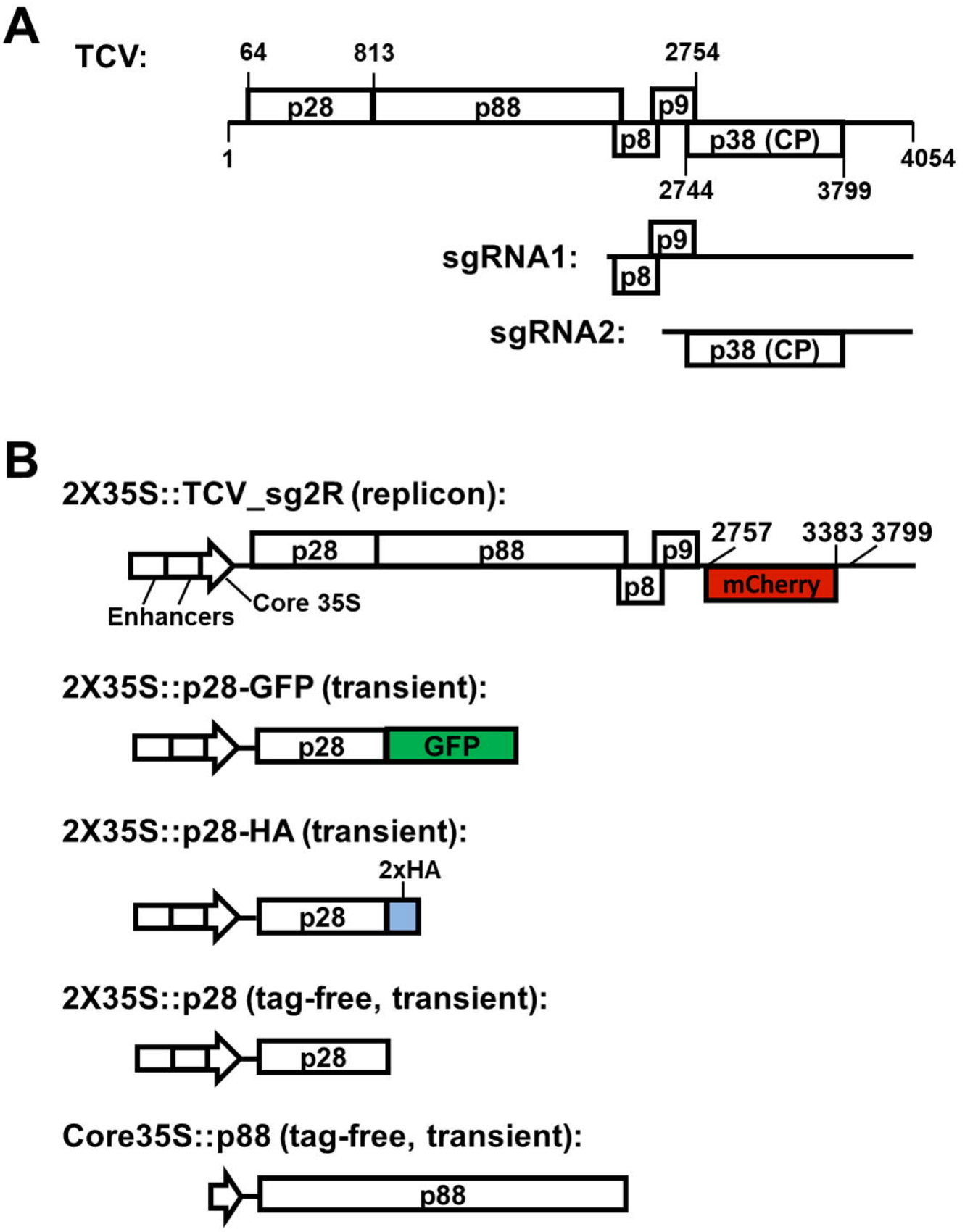

Guo et al., 2019 Fig. 2

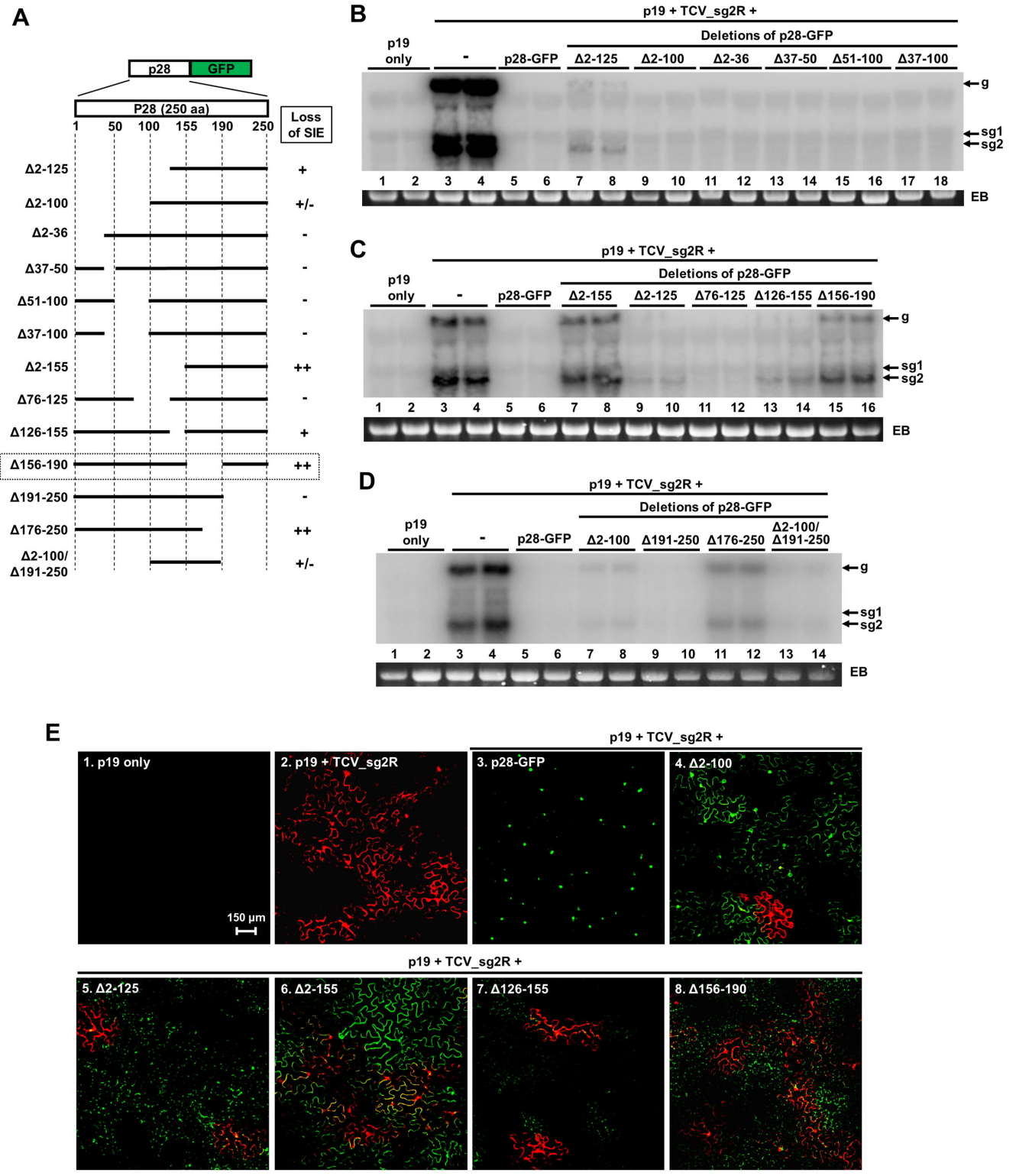

Guo et al., 2019 Fig. 3

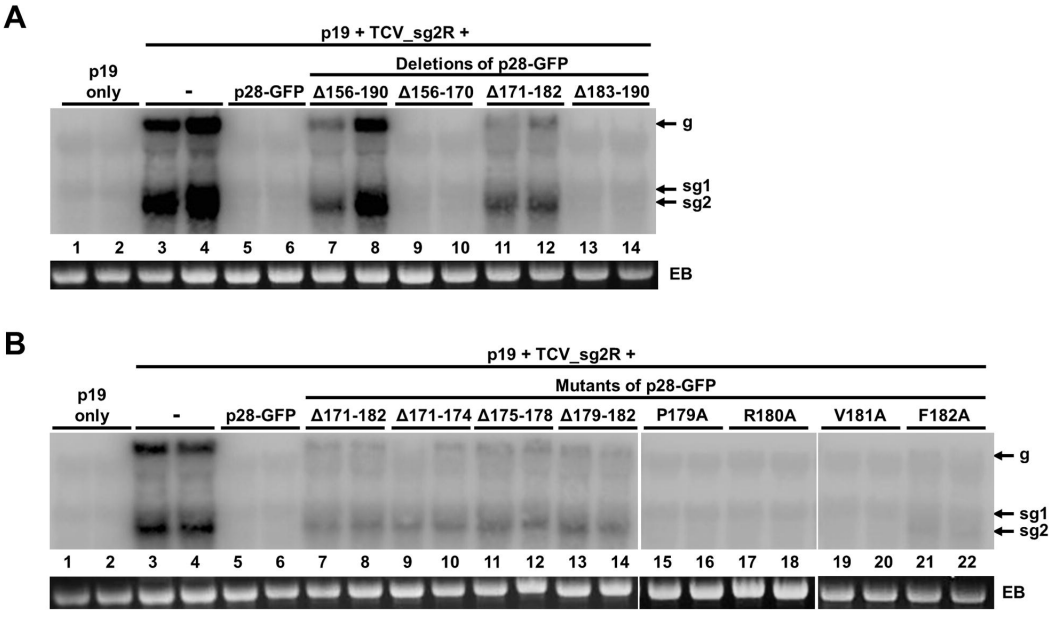

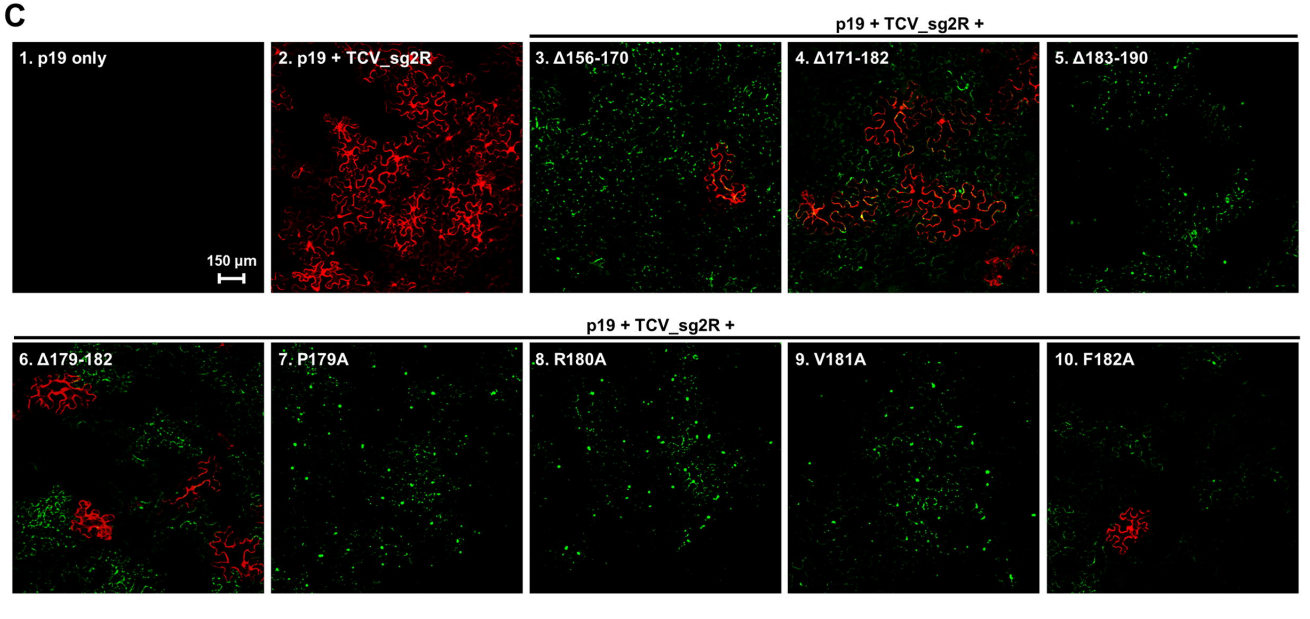

Guo et al., 2019 Fig. 4

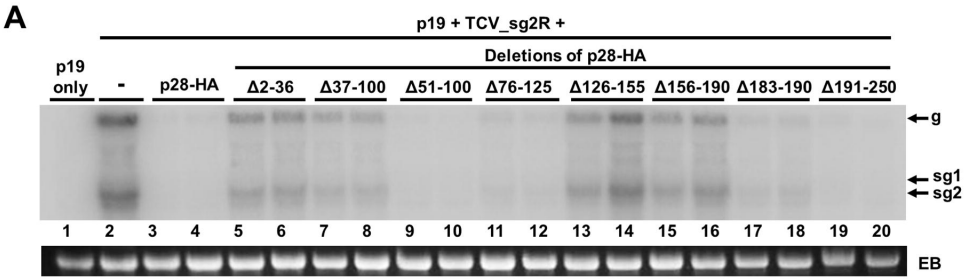

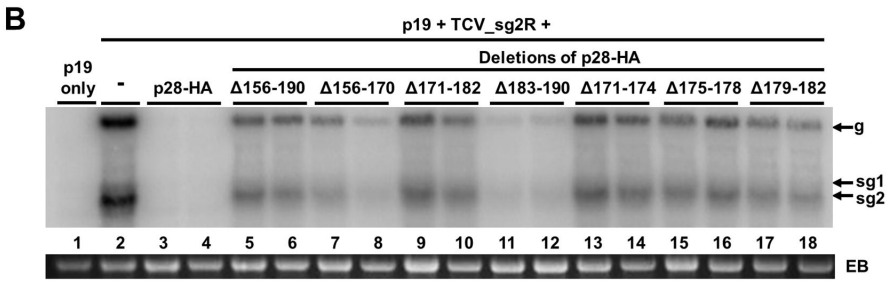

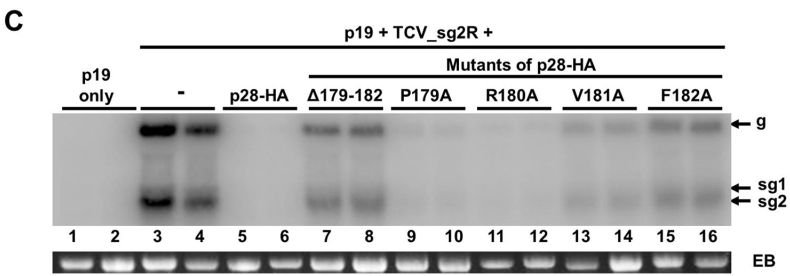

Guo et al., 2019 Fig. 5

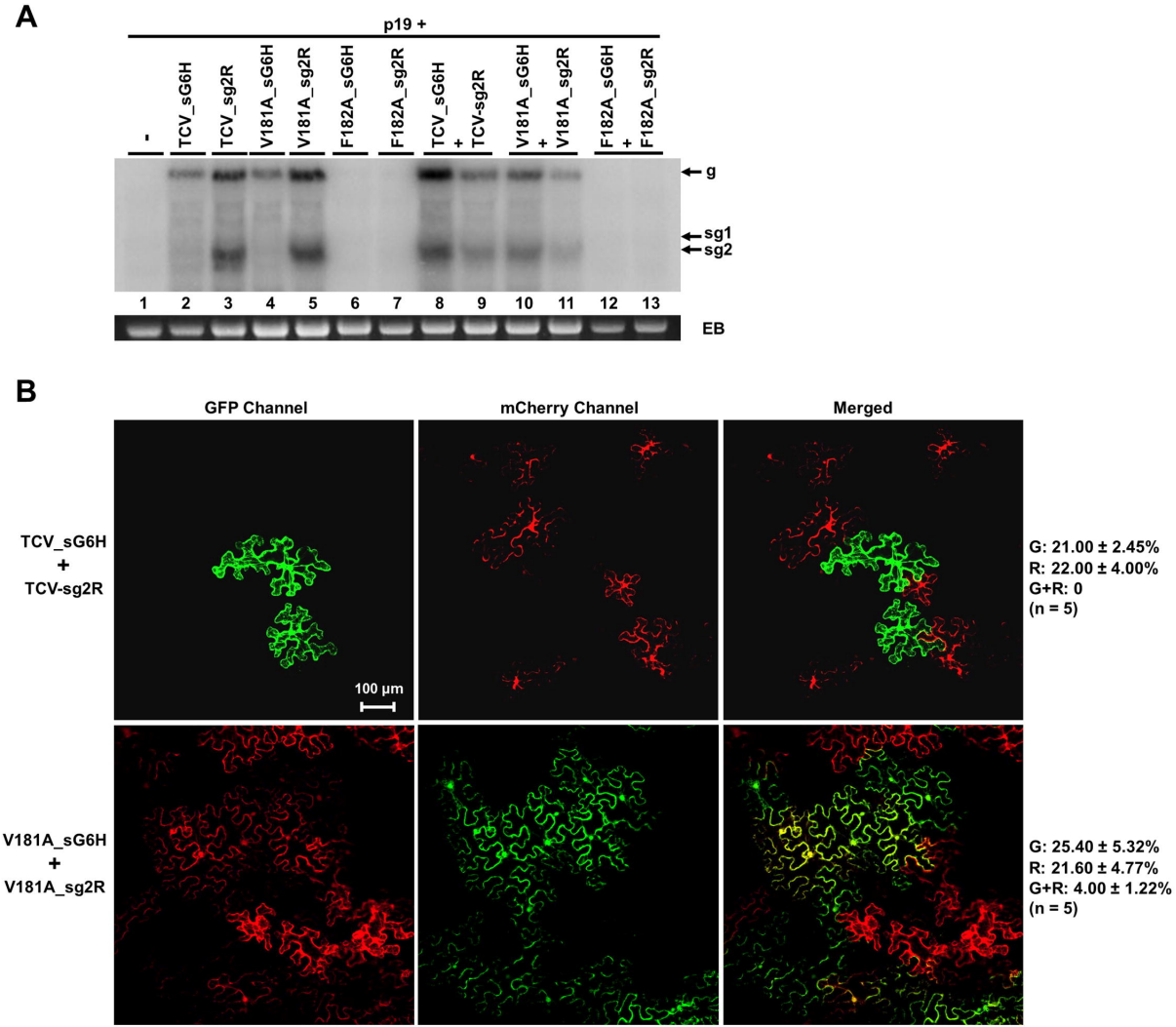

Guo et al., 2019 Fig. 6

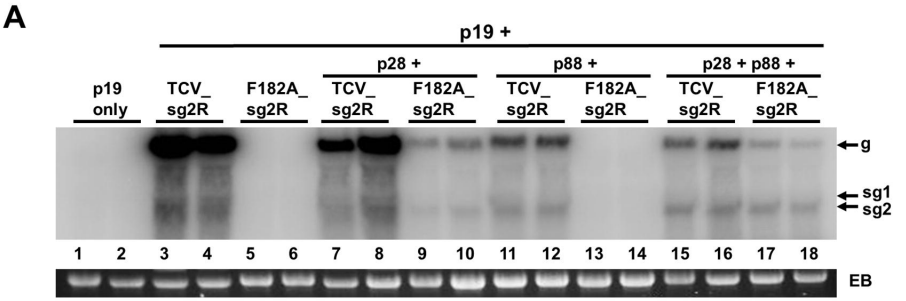

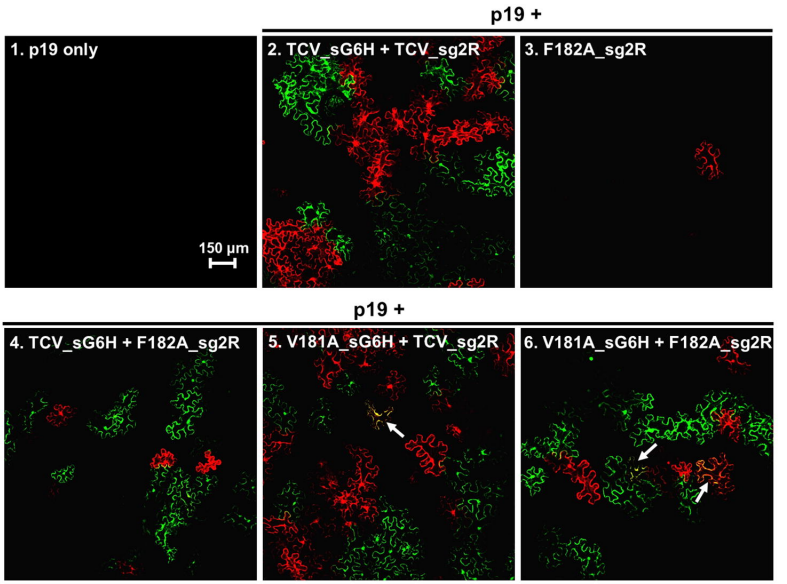

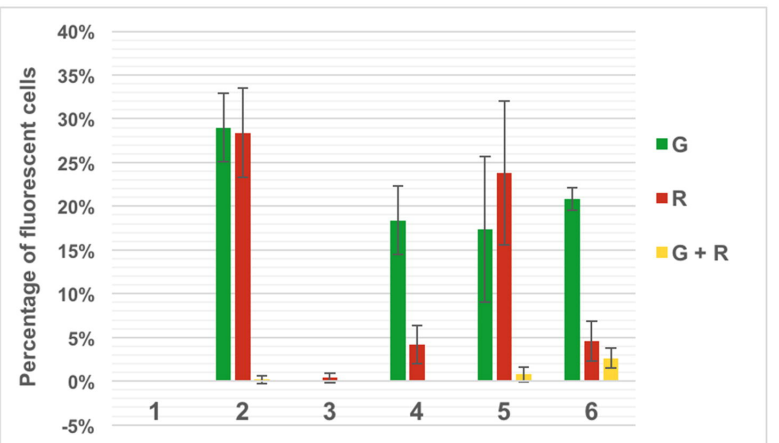
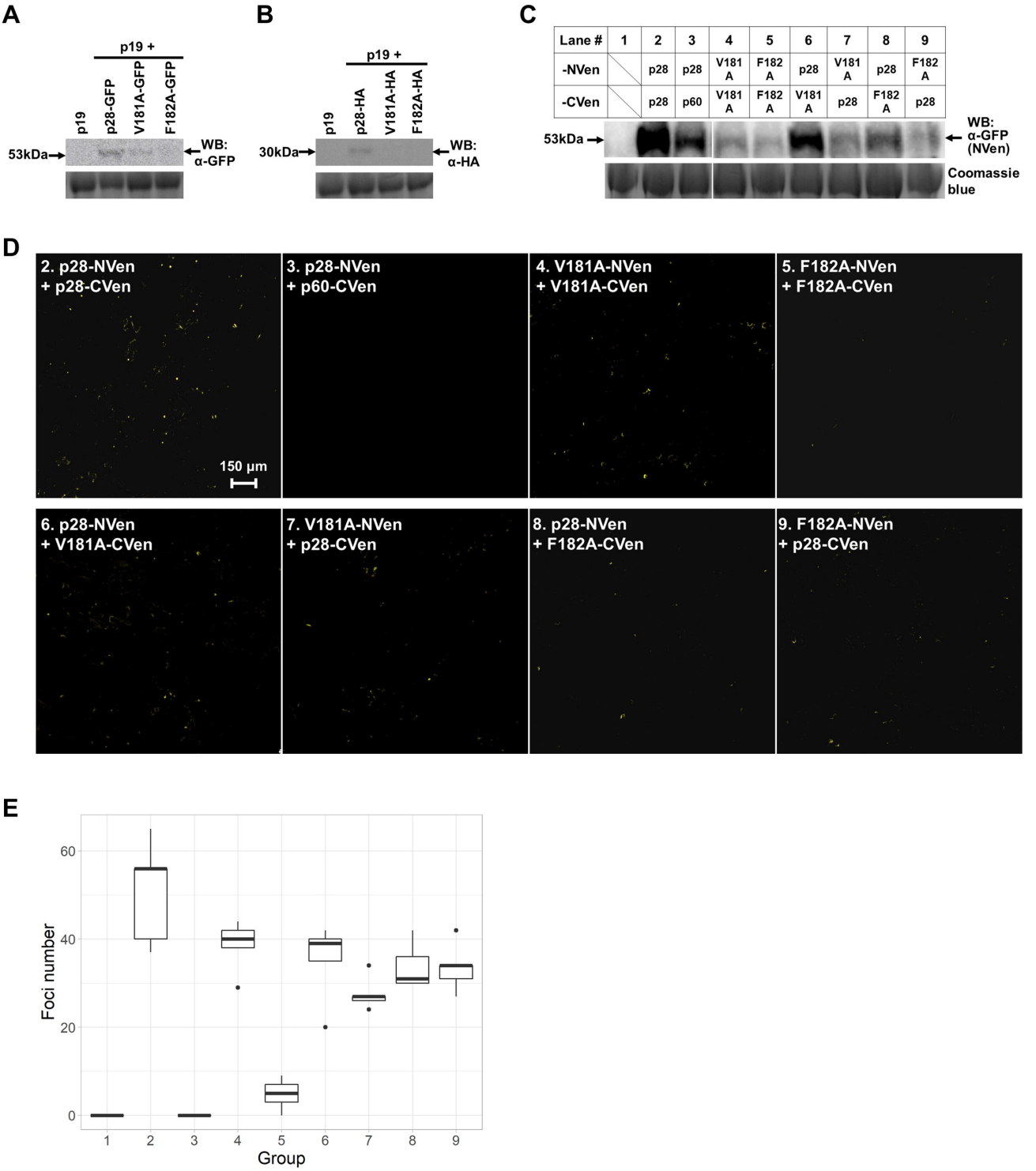
Guo et al., 2019 Fig. 7